British Journal of Pharmacology

British Journal of Pharmacology (2018) **175** 501–516 501

RESEARCH PAPER

4-Aminopyridine: a pan voltage-gated potassium channel inhibitor that enhances K_v7.4 currents and inhibits noradrenaline-mediated contraction of rat mesenteric small arteries

Correspondence Dr Thomas A. Jepps, Department of Biomedical Sciences, Faculty of Health and Medical Sciences, University of Copenhagen, Copenhagen, Denmark. E-mail: tjepps@sund.ku.dk

Received 23 March 2017; **Revised** 1 November 2017; **Accepted** 8 November 2017

Makhala M Khammy[1,2], Sukhan Kim[2], Bo H Bentzen[1], Soojung Lee[3], Inyeong Choi[3], Christian Aalkjær[1,2] and Thomas A Jepps[1]

[1]Department of Biomedical Sciences, Faculty of Health and Medical Sciences, University of Copenhagen, Copenhagen, Denmark, [2]Department of Biomedicine, Aarhus University, Aarhus, Denmark, and [3]Department of Physiology, Emory University School of Medicine, Atlanta, GA, USA

BACKGROUND AND PURPOSE

K_v7.4 and K_v7.5 channels are regulators of vascular tone. 4-Aminopyridine (4-AP) is considered a broad inhibitor of voltage-gated potassium (K_V) channels, with little inhibitory effect on K_v7 family members at mmol concentrations. However, the effect of 4-AP on K_v7 channels has not been systematically studied. The aim of this study was to investigate the pharmacological activity of 4-AP on K_v7.4 and K_v7.5 channels and characterize the effect of 4-AP on rat resistance arteries.

EXPERIMENTAL APPROACH

Voltage clamp experiments were performed on *Xenopus laevis* oocytes injected with cRNA encoding KCNQ4 or KCNQ5, HEK cells expressing K_v7.4 channels and on rat, freshly isolated mesenteric artery smooth muscle cells. The effect of 4-AP on tension, membrane potential, intracellular calcium and pH was assessed in rat mesenteric artery segments.

KEY RESULTS

4-AP increased the K_v7.4-mediated current in oocytes and HEK cells but did not affect K_v7.5 current. 4-AP also enhanced native mesenteric artery myocyte K^+ current at sub-mmol concentrations. When applied to NA-preconstricted mesenteric artery segments, 4-AP hyperpolarized the membrane, decreased $[Ca^{2+}]_i$ and caused concentration-dependent relaxations that were independent of 4-AP-mediated changes in intracellular pH. Application of the K_v7 channel blocker XE991 and BK_{Ca} channel blocker iberiotoxin attenuated 4-AP-mediated relaxation. 4-AP also inhibited the NA-mediated signal transduction to elicit a relaxation.

CONCLUSIONS AND IMPLICATIONS

These data show that 4-AP is able to relax NA-preconstricted rat mesenteric arteries by enhancing the activity of K_v7.4 and BK_{Ca} channels and attenuating NA-mediated signalling.

Abbreviations

4-AP, 4-aminopyridine; BK_{Ca}, large-conductance calcium-activated potassium channels; $Ca^{2+}{}_i$, intracellular calcium; K_V channel, voltage-gated potassium channel

 DOI:10.1111/bph.14097

Introduction

4-Aminopyridine (4-AP; IUPAC, pyridine-4-amine; molecular formula: $C_5H_6N_2$) is considered a broad inhibitor of voltage-gated potassium channels (**K_v1–K_v12**) and has been demonstrated to block most known K_v1-K_v4 channel subtypes (Stühmer *et al.,* 1989; Choquet and Korn, 1992; Grissmer *et al.,* 1994; Coetzee *et al.,* 1999; Wulff *et al.,* 2009). The K_v7 family (K_v7.1–K_v7.5; encoded by the KCNQ1–5 genes; Alexander *et al.,* 2017) is proposed to be less sensitive to 4-AP (Robbins, 2001); however, the effect of 4-AP on K_v7 channels has yet to be systematically studied, either in heterologous expression systems or in tissues expressing native channels.

In the vasculature, various K_v channels are known to regulate smooth muscle reactivity and arterial tone. Members of the K_v1 and K_v2 family (Alexander *et al.,* 2017) were previously thought to be the predominating K_v channels (Albarwani *et al.,* 2003; Fergus *et al.,* 2003; Cox *et al.,* 2008); however, more recently K_v7 channels, namely, **K_v7.4** and **K_v7.5**, have been identified as major determinants of vascular tone (Yeung *et al.,* 2007; Mackie *et al.,* 2008; Ng *et al.,* 2011; Mani *et al.,* 2013; Brueggemann *et al.,* 2014; Jepps *et al.,* 2014; Stott *et al.,* 2014). In many studies using arterial segments or isolated smooth muscle cells, 4-AP has been used to differentiate and dissect out the physiological roles of the more sensitive K_v1 and K_v2 channels and the purportedly less sensitive K_v7 channels.

Considering the functional importance of K_v channels in the vasculature and the use of 4-AP as a pharmacological tool, it is important that we fully understand the effect of 4-AP on all physiologically relevant K_v channels, particularly the K_v7 subfamily, to enable correct interpretation of studies using the drug. Therefore, the aim of this study was to investigate any potential pharmacological activity of 4-AP on K_v7.4 and K_v7.5 channels and subsequently characterize the effect of 4-AP on vascular smooth muscle membrane potential, $[Ca^{2+}]_i$, and tone.

Methods

Ethical statement

This study was approved by the National Ethics Committee, Denmark (License no.: 2014-15-2934-0161), and performed in accordance with Directive 2010/63/EU on the Protection of Animals Used for Scientific Purposes and the guidance on design and analysis recommended by the British Journal of Pharmacology (Curtis *et al.,* 2015). Animal studies are reported in compliance with the ARRIVE guidelines (Kilkenny *et al*., 2010; McGrath and Lilley, 2015).

Animals and general experimental methods

Male Wistar rats (10–12 weeks old; Janvier, France) were housed in groups of two to four in high-top cages under constant climatic conditions (22°C, 12 h light/dark cycle) and provided access to food and water *ad libitum*. Rats were killed by cervical dislocation, and the mesenteric vascular bed excised and placed in cold physiological salt solution (PSS; composition in mM: NaCl 121; KCl 2.82; KH_2PO_4 1.18; $MgSO_4.7H_2O$ 1.17; $NaHCO_3$ 25; $CaCl_2$ 1.6; EDTA 0.03; glucose 5.5) saturated with carbogen (O_2 95%; CO_2 5%) at pH 7.4.

Assessment of K_v7 currents in oocytes with two-electrode voltage-clamp

Xenopus laevis oocytes (EcoCyte Bioscience, Castrop-Rauxel, Germany) were injected with cRNA encoding the hK_v7.4 or hK_v7.5 channel. cRNA was prepared from linearized plasmids according to the manufacturer's instructions (mMESSAGE mMACHINE T7 kit; Ambion, TX, USA), and RNA concentrations were quantified by UV spectroscopy (NanoDrop, Thermo Scientific, Wilmington, USA) and quality checked by gel electrophoresis. A total of 50 nL cRNA (0.05 $\mu g \cdot \mu L^{-1}$ hK_v7.4; 0.2 $\mu g \cdot \mu L^{-1}$ hK_v7.5) was injected. After 3 days of incubation at 19°C, currents were recorded using a two-electrode voltage-clamp amplifier (Dagan CA-1B; IL, USA). Data were sampled at 1 kHz. Two intracellular borosilicate glass recording electrodes (Module Ohm, Herlev, Denmark) were pulled on a DMZ-Universal Puller (Zeitz Instruments, Martinsried, Germany) with a resistance of 0.2–1 MΩ when filled with 2 M KCl and inserted into the oocytes. Oocytes were superfused with Kulori solution (mM): NaCl 90, KCl 4, $MgCl_2$ 1, $CaCl_2$ 1, HEPES 5, pH = 7.4, room temperature. The oocytes were voltage-clamped at a holding potential of −80 mV. Two different voltage protocols were used to elicit the K_v7 currents. A voltage step to −20 mV (3 s) was repeatedly used to investigate if steady state current amplitudes had been achieved, and when stable current amplitudes were achieved (3 min), a current–voltage relationship (I/V) protocol was performed. An I/V voltage protocol was used to establish the current–voltage relationship and the voltage dependence of the channel. The I/V protocol consisted of voltage steps (3 s) from −100 to +40 mV in 20 mV increments followed by a step back to −30 mV (1 s). The solution was subsequently changed to Kulori solution containing increasing concentrations of 4-AP (0.1, 1 and 5 mM), each titrated to a pH of 7.4. At each concentration, an I/V protocol was performed when steady state current levels had been achieved.

Data acquisition was performed with the Pulse software (HEKA Elektronik, Germany), and data analysis was performed using Igor Pro (Wavemetrics, USA) and Graphpad prism (GraphPad Software Inc., USA). Current voltage relationships were generated by measuring the mean current amplitude at the end of the depolarizing step and plotting this against the test potential. Peak tail currents were recorded immediately upon changing the membrane potential to −30 mV. To establish the voltage-dependence of channel activation, the peak currents measured were normalized to the maximum tail current (I/Imax). The normalized tail current was then plotted against the preceding test potential. The tail current–voltage relationship was then fitted to a Boltzmann equation.

Measurement of pH_i in oocytes

Oocyte pH_i was measured as described previously (Lee *et al*., 2014). Briefly, an oocyte was impaled with (i) a pH electrode containing the hydrogen ionophore 1 cocktail B (Sigma-Aldrich, cat #: 95293) back-filled with the phosphate buffer and (ii) a Vm electrode containing 3 M KCl to monitor a membrane potential. The pH electrode was connected to the electrometer FD-223 (World Precision Instruments; Sarasota, FL, USA) routed to a custom-built subtraction amplifier. The Vm electrode was connected to an OC-725C oocyte clamp amplifier (Warner Instrument; Hamden, CT). Another electrode was placed in the bath for reference. Signals from pH and Vm electrodes were collected by a Digidata 1322A (Molecular Sunnyvale, CA, USA) and analysed using pClamp (Molecular Devices). The signal from the pH electrode was subtracted from that of the Vm electrode, and the slope of signal to pH (typically 55 ± 4 mV/pH) was determined using pH 6.0 and 8.0 standards. Measurements were performed at room temperature.

HEK cell electrophysiology

Monoclonal HEK293 cells stably expressing human $K_v7.4$ channels were grown in DMEM, supplemented with 10% FBS (Th Geyer, Denmark) supplemented with Glutamax (Substrate Department, the Panum Institute, Copenhagen, Denmark) and incubated at 37°C in 5% CO_2. K^+ currents were recorded from these cells using a QPatch 16 HT automated patch clamp system (Sophion-Bioscience, Denmark), as previously described (Jepps *et al.,* 2014). The extracellular solution contained the following (in mM): 145 NaCl, 1 $MgCl_2$, 2 $CaCl_2$, 10 HEPES, 4 KCl and 10 glucose (pH 7.4). The intracellular solution contained (in mM): 1.75 $MgCl_2$, 10 EGTA, 110 KCl, 5.4 $CaCl_2$ and 4 Na_2-ATP (pH 7.4). $K_v7.4$ currents were elicited every 5 s by depolarizing the membrane potential to 0 mV for 500 ms from a holding potential of −80 mV. After 2 min of stabilization, increasing concentrations of 4-AP were added, and the current at 0 mV was determined. An I/V protocol was performed on control currents and in the presence of 0.1 and 5 mM 4-AP. The I/V protocol stepped from −100 to +60 mV (20 mV increments, 500 ms duration) returning to −30 mV to measure the tail current.

Perforated patch clamp experiments on isolated mesenteric artery smooth muscle cells

Third-order mesenteric arteries were placed in a smooth muscle dissection solution (SMDS) containing (in mM): 60 NaCl, 80 sodium glutamate, 5 KCl, 2 $MgCl_2$, 10 glucose and 10 HEPES (pH 7.4) at 37°C for 10 min. A two-step, enzymatic dispersal of single myocytes was performed. Vessels were initially incubated in SMDS containing BSA (1 mg mL^{-1}, Sigma, Missouri, USA), papain (0.5 mg mL^{-1}; Sigma, Missouri, USA) and dithiothreitol (1.5 mg mL^{-1}) at 37°C for 8–10 min, before being incubated in SMDS containing 100 μmol L^{-1} Ca^{2+}, BSA (1 mg mL^{-1}) and collagenase (0.7 mg mL^{-1} type F and 0.4 mg mL^{-1} type H; Sigma, MO, USA) at 37°C for 8–10 min. The vessels were then washed in ice-cold SMDS, and single myocytes were liberated by gentle trituration with a fire-polished pipette. Cells were kept in ice-cold SMDS to be used within 5 h.

Membrane current recordings were made using β-escin (50 μmol L^{-1}, Sigma, MO, USA) perforated-patch technique in voltage-clamp mode. Fire-polished patch pipettes had a resistance of 3–6 MΩ when filled with a pipette solution of (mM): K^+ gluconate (110), KCl (30), $MgCl_2$ (0.5) HEPES (5) and EGTA (0.1), pH 7.3. The external solution contained (mM): NaCl (145), KCl (4), $MgCl_2$ (1), $CaCl_2$ (2), HEPES (10) and glucose (10), pH 7.4. **Nicardipine** (0.1 μM) was added to the external solution to prevent the opening of voltage-gated Ca^{2+} channels and smooth muscle cell contraction. Control I/Vs were determined from a holding potential of −80 mV using a step protocol with +10 mV steps to a maximum potential of 50 mV, with 750 ms duration, returning to −30 mV to measure the tail current. For each test potential, the end-pulse current amplitude was taken. Test pulses from −60 to −20 mV were then run every 20 s. After three stable control currents, either 1 μM **XE991** or 0.1 mM 4-AP was perfused into the bath, and changes were monitored with the test pulses. After 3 min an I/V was performed. Following the application of XE991 to the cells, the test pulse and I/V protocols were repeated with 0.1 mM 4-AP added to the perfusate. The electrical signals were recorded using an Axopatch 700B patch clamp amplifier (Molecular Devices, Sunnydale, CA, USA) generated and digitized using a Digidata 1322A hosted by a PC running pClamp 10.4 software (Molecular Devices, Sunnydale, CA, USA).

Measurements of isometric force in arteries

Third-order mesenteric arteries (2 mm length; internal diameter = 256 ± 5 μm) were isolated and mounted on 40 μm stainless steel wires in isolated chambers of a multi wire myograph system [model 620 M, Danish Myo Tehcnology (DMT), Aarhus, Denmark] containing PSS thermoregulated to 37°C and saturated with carbogen (O_2 95%; CO_2 5%; pH 7.4). Each artery segment was normalized by a passive stretch-tension protocol to ensure optimal force development as previously described (Mulvany and Halpern, 1977). Briefly, each artery segment was stretched to 0.9 times the estimated internal circumference when under a transmural pressure of 100 mmHg. After equilibrium, the viability of arterial segments was assessed by stimulation with a high potassium solution (KPSS: PSS with an equimolar substitution of KCl for NaCl; 125 mM K^+) containing **NA** (10 μM). Arterial segments were also stimulated with KPSS to establish a reference maximal contraction. In some arteries, the endothelium was mechanically removed by introducing a hair into the lumen of the mounted artery. To assess endothelium integrity, carbachol (1 μM) was added to arteries precontracted with NA (3 μM). Successful removal of the endothelium was confirmed if the relaxation to carbachol was <10% of precontraction. Arteries were subsequently equilibrated for a further 20 min in PSS prior to any experimental protocol. Force (mN) was recorded with a Powerlab 8/25-LabChart 7 Pro data acquisition system (AD Instruments Ltd., Oxford, UK).

To assess the functional effect of 4-AP, cumulative concentration–response curves to 4-AP (0.1–5 mM) were generated in arteries under passive tension or precontracted with one of the following: (i) NA, to approximately 90% of the KPSS-induced maximal contraction; (ii) 62 mM KPSS (+ 0.1 μM **prazosin** to inhibit the effect of endogenous NA); or (iii) 125 mM KPSS with 10 μM NA [following pretreatment with **guanethidine** (60 min) to prevent the release of endogenous NA]. Concentration–response curves to 4-AP were generated in the presence of (i) DMSO (0.1%: Control); (ii) XE991 (1 μM); (iii) **iberiotoxin** (0.1 μM); and (iv) a combination of (ii) and (iii). In other experiments, 4-AP-mediated vasorelaxation was assessed in NA-precontracted arteries where the endothelium was removed. Concentration-relaxation-response curves were also generated to the **K_{ATP}** (K_{ir}6.2) channel opener, **pinacidil**, in NA–precontracted arteries in the absence and presence of 1 μM XE991. We further generated concentration–response curves to NA in the absence and presence of (i) 1 mM 4-AP; (ii) 1 μM XE991 and 0.1 μM iberiotoxin; and (iii) 1 mM 4-AP, 1 μM XE991 and 0.1 μM iberiotoxin.

Simultaneous measurement of isometric force and $[Ca^{2+}]_i$

Artery segments (2 mm) were mounted in a single chamber confocal myograph system (360CW model, DMT) and equilibrated, normalized and activated as per the standard protocol described earlier. Arteries were loaded with 5 μM of the ratiometric Ca^{2+} indicator Fura-2AM (Life Technologies Europe BV, Naerum, Denmark) dissolved in a load mix composed of 0.04 g Pluronic F-127 (Life Technologies Europe BV) and 200 μL of Cremophor EL (Sigma-Aldrich, Brøndby, Denmark) in 1 mL DMSO for two 30 min periods in PSS. The final concentration of DMSO and Cremophor EL in the bath was 0.08% (vv^{-1}) and 0.02% (vv^{-1}) respectively. Arteries were subsequently washed and excited alternately with wavelengths of 350 and 380 nm using a Zeiss Axiovert 135 microscope equipped with a TILL Photonics Polychrome Illuminator (Till Photonics, Germany) and a 40× water immersion objective (Zeiss). Emission from the preparation was collected with a >510 nm cut-off filter. Images were acquired using a CoolSNAP CCD camera (Photometrics, Tuscan, AZ, USA) and recorded with Metafluor Fluorescence Ratio Imaging Software (Molecular Devices, Berkshire, UK). The intensity ratio (F_{350}/F_{380}) was calculated after subtraction of background fluorescence acquired prior to Fura-2AM addition.

Simultaneous measurement of isometric force and pH_i

In some arteries, isometric force was measured simultaneously with pH_i. Arteries were loaded with 5 μM of the ratiometric pH-sensitive fluorophore 2′,7′-bis-(2-carboxyethyl)-5-(and-6)-carboxyfluorescein (BCECF-AM; Life Technologies) in 0.1% DMSO in PSS for 5 min before excess dye was washed out. Arteries were excited at alternating wavelengths (440 and 495 nm) and emission collected with a >510 nm cut-off filter using a Leica DM IRB inverted microscope (Ballerup, Denmark) with a ×20 objective (N.A. 0.5.) connected to a Photon Technology International Deltascan system (PTI; Birmingham, NJ, USA) and recorded using FeliX32 Spectroscopy Software (PTI). The intensity ratio (F_{495}/F_{440}) was calculated after subtraction of background fluorescence acquired prior to BCECF-AM addition. Calibration of the intensity ratio was made using K^+-HEPES solution (composition in mM: NaCl 11; $MgSO_4.7H_2O$ 1.2; KCl 132.8; glucose 5.5; EDTA 0.03; KH_2PO_4 1.18; $CaCl_2.H_20$ 1.6; HEPES 10 mM and probenecid 5 mM; bubbled with air) of various pH levels (6.8–8.0) containing the K^+-H^+ ionophore nigericn (10 μM; Sigma) as described previously (Thomas *et al.,* 1979). A mean calibration curve for the intensity ratio was generated from two separate experiments and fitted with least-squares regression (correlation coefficient 0.998).

Following fura-2AM or BCECF-AM loading, artery viability was reassessed with the standard KPSS protocol. After KPSS washout, 1 mM 4-AP was applied at rest for 2 min (protocol i). After washout, arteries were precontracted with 1 μM NA where upon reaching a plateau, 1 mM 4-AP was applied to the preparation (protocol ii). To determine if 4-AP-induced relaxation was occurring via a pH-dependent pathway, we developed a protocol that prevented 4-AP-mediated elevation in pH_i. Briefly, arteries were incubated with NH_4Cl (2 mM) and stimulated with 1 μM NA. When the contractile response to NA had plateaued, PSS in the chamber was replaced with PSS containing 1 μM NA and 1 mM 4-AP. In this manner, only NH_4Cl is washed out. Washout of NH_4Cl is known to elicit acute acidification (Aalkjaer and Cragoe , 1988), and we found that washout of 2–3 mM of NH_4Cl prevented 4-AP-induced alkalization, enabling us to investigate pH_i-independent effects of 4-AP in the absence (protocol iii) and presence of XE991 (1 μM; protocol iv) and in the presence of both XE991 (1 μM) and iberiotoxin (0.1 μM; protocol v). To ascertain the contribution of 4-AP-induced pH_i changes to the inhibition of NA-induced signalling, the NH_4Cl washout protocol was also used to prevent 4-AP-induced pH_i changes in arteries precontracted with 125 mM KPSS and NA (10 uM).

Simultaneous measurement of isometric force and membrane potential

Membrane potentials were measured with sharp glass electrodes as previously described (Mulvany *et al.,* 1982). After the artery segments had been mounted in custom-made myographs and the diameter normalized, measurements were made using aluminium silicate microelectrodes with a resistance of 40–120 MΩ when filled with 3 M KCl. The potentials were recorded with an Intra-767 amplifier (WPI) and visualized on an oscilloscope. Electrode entry into smooth muscle cells was achieved from the adventitial side and resulted in a sudden drop in voltage and a sharp return to baseline when the electrode was retracted.

Data and statistical analyses

In the two-electrode voltage clamp experiments and HEK cell patch-clamp experiments, a Bonferroni *post hoc* test was performed following a two-way ANOVA to compare the effects of different 4-AP concentrations to control currents. A one-way ANOVA followed by a Dunnett's multiple comparisons test was performed to compare V½ values of 4-AP to control. In the patch-clamp experiments on isolated mesenteric artery smooth muscle cells, control and 0.1 mM 4-AP currents were compared by two-way ANOVA followed by a Bonferroni *post hoc* test. Currents recorded in the presence of XE991, 4-AP and XE991 + 4-AP were compared by a two-way ANOVA followed by a Dunnett's multiple comparisons test. The normalized currents at 0 mV of the aforementioned groups were compared by one-way ANOVA followed by a Sidak's multiple comparisons test.

For cumulative concentration–response curves to 4-AP and NA, force data (mN) were expressed as tension (Nm^{-1}) by dividing the force (mN) by twice the artery segment length (mm) and subtracting passive tension values. Data are expressed as mean tension ± SEM. Concentration-relaxation response curves were fitted for each individual experiment using four-parameter nonlinear regression with variable slope and a minimum constrained to >0. From these curves, the EC_{50} (concentration of agonist required to elicit 50% of the maximum response), pEC50 ($-logEC_{50}$) and the maximum relaxation response (Rmax) were derived, unless otherwise stated. For concentration-contraction response curves, only the maximum contractile response (Emax) was determined. For experiments assessing relaxation, pEC_{50}, Rmax and Emax were compared between groups using one-way ANOVA with Dunnett's *post hoc* test for multiple comparisons, unless otherwise specified. For experiments involving the simultaneous measurement of force and $[Ca^{2+}]_i$ or pH_i, 4-AP-mediated responses were expressed as a change from NA-mediated responses: statistical comparisons are indicated in the figure legends. $P < 0.05$ was considered statistically significant and n refers to the number of arteries from separate rats. Statistical analyses were performed using GraphPad Prism 5 (GraphPad Software., San Diego, CA, USA). The data and statistical analysis comply with the recommendations on experimental design and analysis in pharmacology (Curtis *et al.,* 2015).

Materials

Drugs and suppliers were as follows: 4-AP (Sigma-Aldrich, Brøndby, Denmark); carbachol (Sigma-Aldrich); guanethidine sulphate (Sigma-Aldrich); iberiotoxin (Tocris; Bristol, UK); L-(−)-noradrenaline (+)-bitartrate salt monohydrate (Sigma-Aldrich); Pinacidil monohydrate (Sigma-Aldrich); prazosin hydrochloride (Sigma-Aldrich); and XE991 (Sigma-Aldrich). Stock solutions were prepared using anhydrous DMSO (Pinacidil and XE991) or distilled water (carbachol, noradrenaline and iberiotoxin) and stored at −20°C until required. A 0.5 M stock of 4-AP was prepared fresh daily with distilled water and pH adjusted to 7.4.

Nomenclature of targets and ligands

Key protein targets and ligands in this article are hyperlinked to corresponding entries in http://www.guidetopharmacology.org, the common portal for data from the IUPHAR/BPS Guide to PHARMACOLOGY (Southan *et al.,* 2016), and are permanently archived in the Concise Guide to PHARMACOLOGY 2017/18 (Alexander *et al.,* 2017).

Results

4-AP enhanced $K_v7.4$ but not $K_v7.5$ currents

Application of 0.1 and 1 mM 4-AP increased the $K_v7.4$ currents in oocytes at +40 mV, and 5 mM 4-AP increased the currents at +20 to +40 mV. Additionally, in the oocytes overexpressing $K_v7.4$ channels, 1 and 5 mM 4-AP caused a significant shift of the voltage-dependence of channel activation with the V½ of activation changing by −5.0 ± 1.6 mV (n = 5) and −5.2 ± 1.1 mV (n = 5) respectively (Figure 1A; Table 1). In contrast, 4-AP had no effect on the current amplitude or V½ of activation of oocytes overexpressing $K_v7.5$ channels (n = 5–6; Figure 1B; Table 2).

4-AP is known to affect intracellular pH of mammalian cells; therefore, we determined whether oocytes were subject to the same intracellular pH changes. Figure 1C shows that 4-AP was unable to change the intracellular pH of oocytes at concentrations from 0.1–5 mM. This suggests that the 4-AP-mediated increase in $K_v7.4$ current is pH_i-independent.

4-AP enhanced and inhibited the $K_v7.4$ current in HEK cells

In HEK cells stably expressing $K_v7.4$ channels, currents were enhanced by 0.1 mM 4-AP but inhibited by 5 mM 4-AP (Figure 2A; Table 3). At 0.1 and 0.3 mM, 4-AP enhanced the current at 0 mV (Figure 2A). At 1 mM, 4-AP began to suppress the enhanced currents, returning the current to control levels at 0 mV (Figure 2A). Additional application of 4-AP at 3 and 5 mM inhibited the $K_v7.4$ current (Figure 2A). The voltage-dependence of activation was not affected by either 0.1 or 5 mM 4-AP (Figure 2B; Table 4).

4-AP enhanced K^+ currents in mesenteric artery SMCs

Given the bi-phasic nature of 4-AP in HEK cells and that 0.1 mM was able to increase the $K_v7.4$ currents significantly in these cells, we tested the effect of 0.1 mM 4-AP on K^+ currents from isolated mesenteric artery smooth muscle cells. 4-AP enhanced the K^+ currents at 50 mV (Figure 3A; n = 6 for each group). 4-AP also shifted the voltage-dependence of half maximal activation, recorded at −30 mV, from 2.2 ± 1.0 to −4.6 ± 0.4 mV (Figure 3A, panels iv, v; $P < 0.05$ according to a paired t-test). When the K_v7 channel blocker XE991 (1 μM) was applied, the K^+ currents were inhibited (n = 5; Figure 3B). In the presence of XE991, additional application of 0.1 mM 4-AP further inhibited the K^+ currents (n = 5; Figure 3B, C).

4-AP relaxes and contracts mesenteric arteries

In third-order rat mesenteric arteries preconstricted with NA, 4-AP induced concentration-dependent and endothelium-independent relaxations with a pEC_{50} of 3.2 ± 0.1 (Figure 4A). Maximum relaxations were typically observed at 3 or 5 mM 4-AP. In contrast, 4-AP elicited concentration-dependent contraction in arteries precontracted with 62 mM KPSS (Figure 4B). NA concentration–response curves were performed in the absence and presence of 1 mM 4-AP. In the presence of 1 mM 4-AP, NA potency decreased twofold ($P < 0.05$, n = 5), but the maximum contractile response was unchanged (Figure 4C). In arteries at rest, 4-AP elicited contraction at 5 mM but only in two of six arteries tested (Figure 4D). The presence of 1 μM XE991 increased the propensity of 4-AP to elicit contraction (four out of six arteries) whilst 1 μM XE991 in combination with the BK_{Ca} channel inhibitor iberiotoxin (0.1 μM) enhanced the maximum contractile response to 4-AP (Figure 4D).

4-AP-mediated relaxation was associated with smooth muscle membrane hyperpolarization and decreased $[Ca^{2+}]_i$ in precontracted mesenteric arteries

At rest, the application of 1 mM 4-AP had no effect on resting tone (ΔNm^{-1} = 0.03 ± 0.02) but caused a small transient

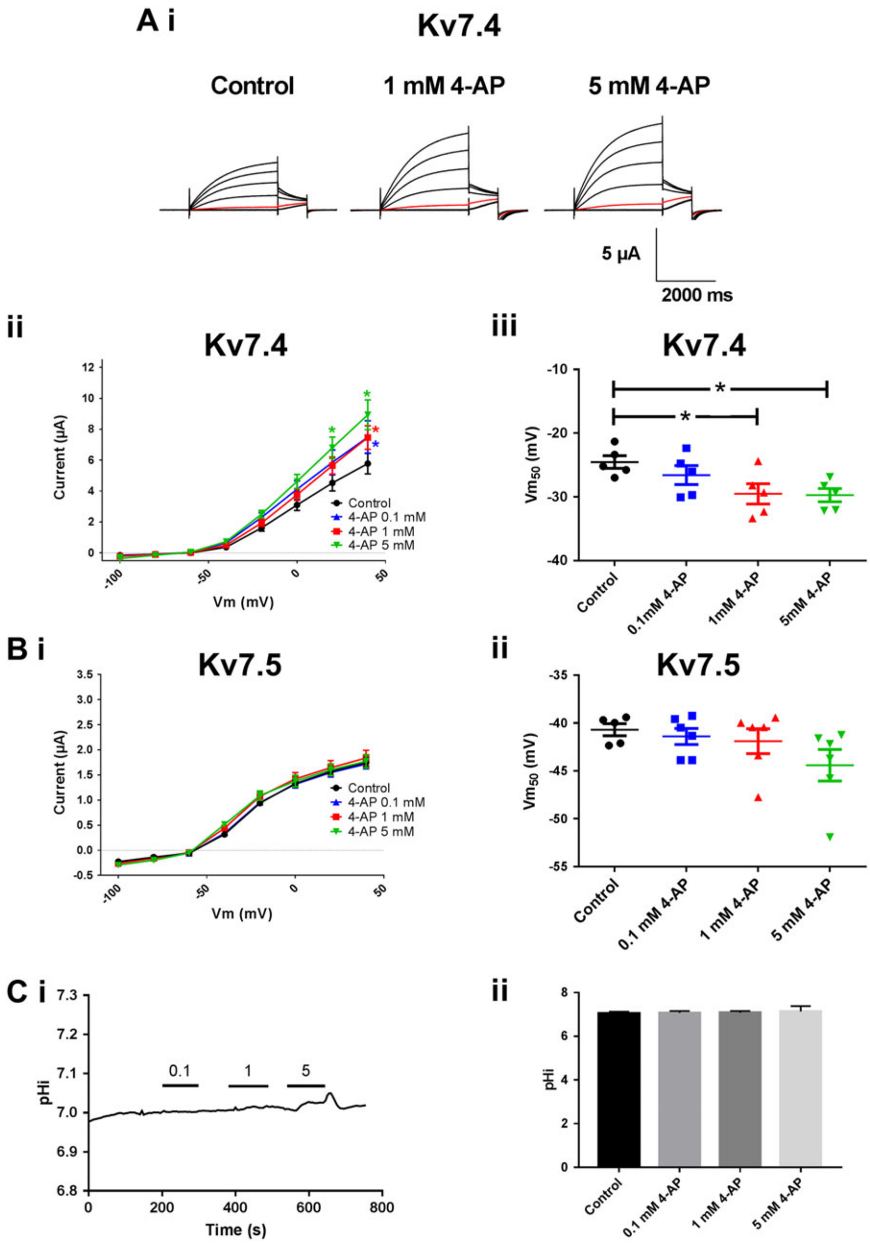

Figure 1

The effect of 4-AP on the hK_v7.4 and hK_v7.5 channels expressed in *Xenopus laevis* oocytes. (A, panel i) Representative K_v7.4 current traces recorded from two-electrode voltage clamp experiments without 4-AP (control; left), after application of 1 mM 4-AP (centre) and after application of 5 mM 4-AP (right). The I/V relationship protocol consisted of voltage steps (3 s) from −100 to +40 mV in 20 mV increments followed by a step back to −30 mV (1 s). Red traces represent the current elicited at −40 mV. Current–voltage relationship comparing the effect of 0.1, 1 and 5 mM 4-AP to control on (Ai) K_v7.4 currents and (Bi) K_v7.5 currents. A Bonferroni *post hoc* test was performed following a two-way ANOVA and *$P < 0.05$. Voltage-dependence of activation curves for (A, panel iii) K_v7.4 and (B, panel ii) K_v7.5 currents was obtained by normalizing the tail current at −30 mV against the maximal tail current measured in each experiment and plotted as a function of the preceding step potential (n = 5–6) and a Boltzmann fit was performed to determine the V½ (Vm_{50}) values plotted. A one-way ANOVA followed by a Dunnett's multiple comparisons test was performed, and *$P < 0.05$. (C, panel i) Representative trace and (C, panel ii) mean intracellular pH measurements in oocytes treated with 0.1, 1 and 5 mM 4-AP.

membrane hyperpolarization in five of seven arteries examined (ΔmV = 2.0 ± 1.1) (Figure 5A, C). There was no effect of 1 mM 4-AP on $[Ca^{2+}]_i$ (ΔFura-2 ratio, 0.001 ± 0.003; n = 10). In mesenteric arteries precontracted with 1 μM NA, the application of 1 mM 4-AP caused a significant and sustained hyperpolarization (17.0 ± 3.2 mV; $P < 0.05$, $n = 6$) that was associated with a simultaneous decrease in tension (0.71 ± 0.22 Nm^{-1}; $P < 0.05$, Student's paired t-test; Figure 5B, D). The relaxation and hyperpolarization of the smooth muscle was associated with a decrease in $[Ca^{2+}]_i$ as indicated by a decrease in the Fura-2 ratio (0.14 ± 0.03, $P < 0.05$; Figure 6).

Table 1

$K_v7.4$ currents from oocytes – Boltzmann fit parameters of tail currents

	Control	4-AP 0.1 mM	4-AP 1 mM	4-AP 5 mM
Bottom	0.059 ± 0.008	0.035 ± 0.03	0.055 ± 0.01	0.064 ± 0.009
Top	0.99 ± 0.009	0.98 ± 0.03	0.99 ± 0.01	0.99 ± 0.009
V_{50}	−24.59 ± 0.61	−24.64 ± 2.25	−29.67 ± 0.82	−29.72 ± 0.65
Slope	11.07 ± 0.55	12.61 ± 2.06	11.19 ± 0.72	10.66 ± 0.55

Table 2

$K_v7.5$ currents from oocytes – Boltzmann fit parameters of tail currents

	Control	4-AP 0.1 mM	4-AP 1 mM	4-AP 5 mM
Bottom	0.31 ± 0.01	0.3 ± 0.02	0.31 ± 0.02	0.32 ± 0.02
Top	0.96 ± 0.01	0.96 ± 0.01	0.97 ± 0.01	0.95 ± 0.01
V_{50}	−40.28 ± 0.99	−41.19 ± 0.96	−42.3 ± 1.33	−43.76 ± 1.91
Slope	5.84 ± 1.81	5.5 ± 1.8	5.97 ± 1.79	4.62 ± 2.01

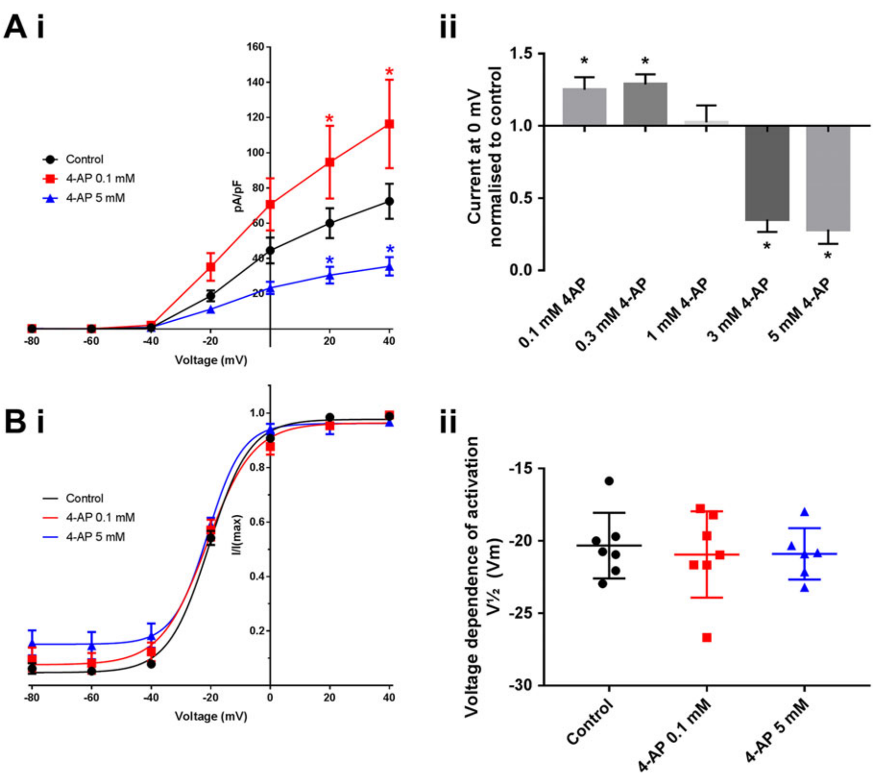

Figure 2

The effect of 4-AP on the $hK_v7.4$ channel expressed in HEK cells. (A, panel i) Current–voltage relationship comparing the effect of 0.1 mM and 5 mM 4-AP to control currents. A Bonferroni *post hoc* test was performed following a two-way ANOVA and $*P < 0.05$. (A, panel ii) The $K_v7.4$ current at 0 mV normalized to control comparing the effects of 0.1–5 mM 4-AP. A Dunnett's multiple comparison test was performed and $*P < 0.05$. (B) Comparison of the voltage-dependence of activation between control, 0.1 and 5 mM 4-AP.

Table 3

K_v7.4 currents from HEK cells – Boltzmann fit parameters of I/V

	Control	4-AP 0.1 mM	4-AP 5 mM
Bottom	0.036 ± 0.01	0.021 ± 0.11	0.049 ± 0.02
Top	0.98 ± 0.01	1.4 ± 0.11	0.42 ± 0.02
V_{50}	−20.23 ± 0.66	−20.97 4.23	−20.96 ± 2.64
Slope	6.56 ± 0.99	8.16 ± 4.71	5.39 ± 5.42

Table 4

K_v7.4 currents from HEK cells - Boltzmann fit parameters of tail currents

	Control	4-AP 0.1 mM	4-AP 5 mM
Bottom	0.047 ± 0.01	0.076 ± 0.02	0.15 ± 0.24
Top	0.98 ± 0.01	0.96 ± 0.02	0.96 ± 0.02
V_{50}	−20.6 ± 0.56	−21.25 ± 1.28	−20.99 ± 1.14
Slope	6.876 ± 0.76	7.77 ± 1.46	5.84 ± 2.02

K_v7 channels partially mediate 4-AP-induced vasorelaxation

Based on the electrophysiological data in Figure 1, we tested whether 4-AP-induced vasorelaxation was due to activation of vascular K_v7.4 channels. XE991 (1 μM) partially inhibited the 4-AP-mediated fall in $[Ca^{2+}]_i$ in NA contracted arteries ($P < 0.05$, Student's paired *t*-test, $n = 7$; Figure 6). Furthermore, 1 μM XE991 caused a rightward shift of the 4-AP concentration–response curve ($P < 0.05$, $n = 6$; Figures 7A–C). Because XE991 may functionally antagonize 4-AP-mediated relaxation by facilitating membrane depolarization and potentiating contractile responses, the concentration of NA was always titrated to achieve approximately 90% of the KPSS-induced contraction. Furthermore, we assessed whether another potassium channel opener would be similarly inhibited by XE991. However, 1 μM XE991 had no effect on the concentration-relaxation response curve to pinacidil, a K_{ATP}-channel opener (Figure 7D).

Both K_v7 and BK_{Ca} activation contribute to 4-AP-mediated relaxation

4-AP has been shown previously to activate **BK_{Ca}** (K_{Ca}1.1) channels (Petkova-Kirova *et al.,* 2000). In NA-preconstricted mesenteric artery segments, pretreatment of arteries with iberiotoxin (0.1 μM) significantly decreased the Rmax (97 ± 2% to 72 ± 13%, $n = 7$; Figure 7A, C) of 4-AP but did not alter potency (Figure 7B). In the presence of 1 μM XE991, 0.1 μM iberiotoxin strongly inhibited 4-AP-mediated relaxation (Rmax, 35 ± 8%; $P < 0.05$, $n = 6$; Figure 7A, C). XE991 and iberiotoxin, alone, did not alter the basal tension of mesenteric arteries but generated substantial tone when combined (0.80 ± 0.20 Nm^{-1}). Notably, the level of NA-induced precontraction was similar irrespective of pretreatment. The tension developed by NA in DMSO-, XE991-, IBTx- or XE991 + IBTx-treated arteries was 2.31 ± 0.21, 2.36 ± 0.16, 2.58 ± 0.23 and 2.27 ± 0.22 Nm^{-1} respectively.

4-AP increased pH_i in mesenteric arteries

Previously, 4-AP was shown to enhance BK_{Ca} currents in vascular smooth muscle cells via an increase in pH_i (Petkova-Kirova *et al.,* 2000). To investigate whether increases in pH_i were responsible for the 4-AP-mediated relaxations, we measured pH_i and tension simultaneously in intact isolated mesenteric arteries. Addition of 1 mM 4-AP to arteries in PSS caused a sustained alkalization (0.15 ± 0.02 pH units, $n = 6$) but no change in tension. Sustained alkalization (0.19 ± 0.03 pH units, $n = 9$) was also observed with 1 mM 4-AP when applied to arteries precontracted with NA (Figure 8A), which was accompanied by almost complete relaxation (89.7 ± 5.3% of NA precontraction).

4-AP-mediated relaxation occurs via pH_i-dependent and independent mechanisms

When 4-AP-mediated alkalization was prevented (Figure 8A, protocol iii) using an NH_4Cl washout protocol (ΔpH_i with 1 mM 4-AP = 0.00 ± 0.03 units, $n = 9$), the magnitude of the relaxation to 1 mM 4-AP was unchanged (86.7 ± 6.4% of NA precontraction, $n = 9$; Figure 8B). Notably, however, the time taken for the 4-AP-mediated relaxation response to plateau was significantly longer when pH_i was maintained at baseline values (286 ± 42 s) compared to control (156 ± 19 s; $P < 0.05$, $n = 8$; Figure 8C). Repeating the NH_4Cl washout protocol in the presence of 1 μM, XE991 (protocol iv) decreased the magnitude of 4-AP-mediated relaxation (60 ± 8%; $P < 0.05$, $n = 8$; Figure 8B) without further lengthening the time taken for the relaxation to plateau (297 ± 30 s; Figure 8C). When the NH_4Cl washout protocol was repeated in the presence of both 1 μM XE991 (1 μM) and 0.1 μM iberiotoxin (protocol v), 4-AP-mediated relaxations were inhibited (18 ± 3% of NA precontraction; $P < 0.05$, $n = 5$; Figure 8B), but the time taken for the relaxation to plateau was not significantly different from control (272 ± 37 s; Figure 8C).

4-AP-mediated relaxation of arteries precontracted with NA occurs via K_v7/BK_{Ca} activation and inhibition of NA-stimulated signalling

4-AP caused concentration-dependent relaxations of arteries precontracted with the combination of 125 mM KPSS and 10 μM NA (Figure 9A). At higher concentrations (≥3 mM), relaxation was transient with tension plateauing slightly above the peak relaxation response (Figure 9A, panel i). Rmax, calculated as a percentage of the contraction induced by10 μM NA on top of 125 mM KPSS, was 75 ± 5%. In arteries precontracted with both 125 mM KPSS and 10 μM NA, the ability of 4-AP to relax the additional NA-induced component was unchanged in the presence of 1 μM XE991 and 0.1 μM iberiotoxin (Supporting Information Figure S1, $n = 5$–8). In arteries precontracted with U46619 in the presence of L-type calcium channel blockade, 4-AP failed to induce any significant relaxation (Supporting Information Figure S2, $n = 8$).

When 4-AP-induced intracellular alkalization was prevented using an NH_4Cl washout protocol, the relaxation response to 1 mM 4-AP in arteries precontracted with both 125 mM KPSS and NA (10 μM) was reduced significantly (Figure 9B).

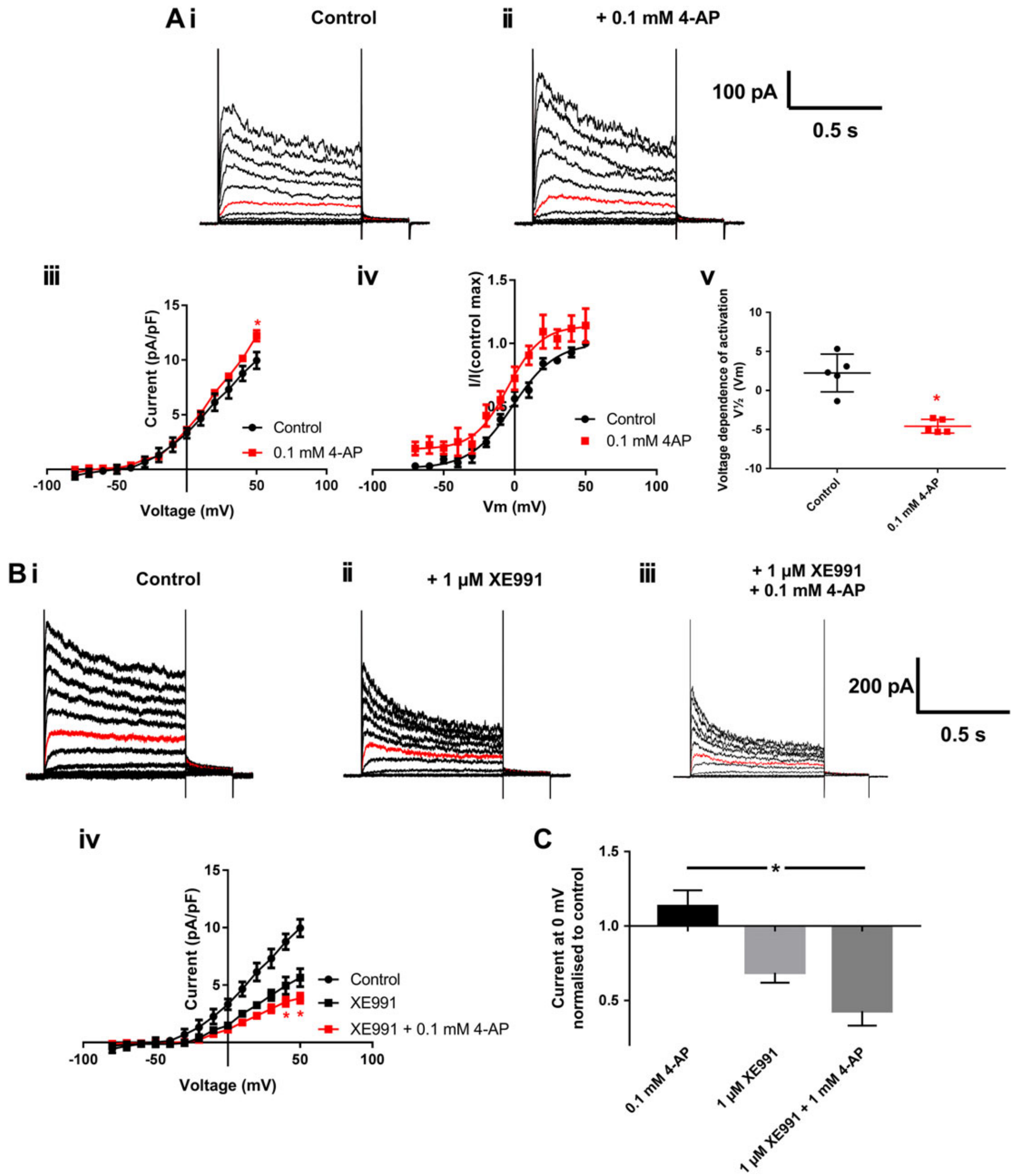

Figure 3

Electrophysiological effects of 4-AP on isolated mesenteric artery smooth muscle cells. (A) Representative currents produced by an I/V protocol from −80 mV to +50 mV stepping up in 10 mV increments for 750 ms (A, panel i) before and (A, panel ii) after application 0.1 mM 4-AP. (A, panel iii) Mean I/V relationship data showing the effect of 0.1 mM 4-AP compared to control currents (*$P < 0.05$ according to a two-way ANOVA followed by a Sidak's multiple comparison test). The effect of 0.1 mM 4-AP was also observed on (A, panel iv) mean tail currents recorded at −30 mV after the voltage steps were plotted and (A, panel v) the half-maximal voltage-dependence of activation calculated in each experiment (*$P < 0.05$ according to a paired *t*-test). (B) Representative currents showing the effect of (B, panel ii) the K_v7 channel blocker XE991 followed by the subsequent application of (B, panel iii) 0.1 mM 4-AP. (B, panel iv) Mean I/V data comparing the effect of 0.1 mM 4-AP to XE991 + 0.1 mM 4-AP (*$P < 0.05$ according to a two-way ANOVA followed by a Sidak's multiple comparison test). The mean control current is added for context. (C) Comparison of the currents produced by 0.1 mM 4-AP, 1 μM XE991 and 1 μM XE991 + 0.1 mM 4-AP at 0 mV normalized to the control current at 0 mV (*$P < 0.05$ following a one-ANOVA and Sidak's multiple comparisons test).

Furthermore, NA concentration–response curves constructed in the presence of 1 μM XE991 and 0.1 μM iberiotoxin were rightward shifted by 1 mM 4-AP (Figure 9C).

To determine the relative contribution of (i) K_v7 channels and BK_{Ca} activation; and (ii) inhibition of NA-mediated signalling, to 4-AP-mediated relaxation of NA-precontracted arteries, data from Figures 4C and 9C are alternatively presented in Figure 9D wherein the ability of 1 mM 4-AP to inhibit NA-mediated constriction (Inhibitory effect of 1 mM 4-AP; Y-axis) is expressed as a function of tension generated by NA (T_{NA}; X-axis). Here, the inhibitory effect of 1 mM

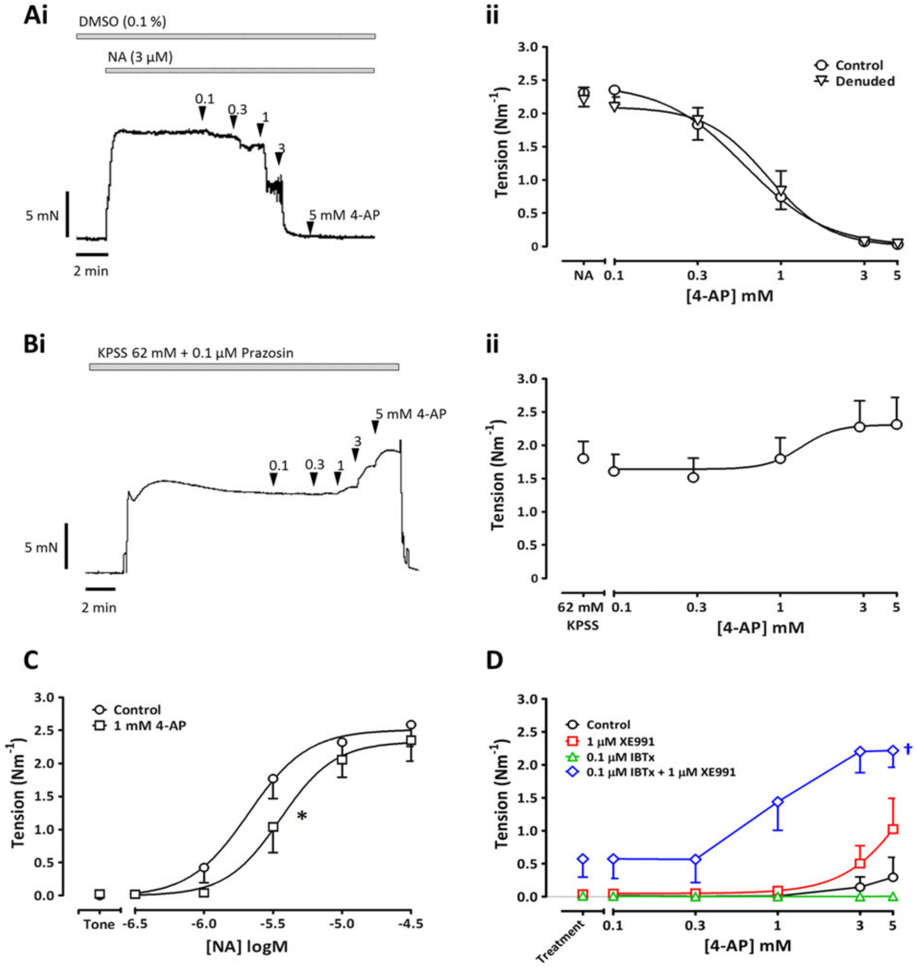

Figure 4

4-AP is able to relax and contract isolated rat mesenteric arteries. (A, panel i) Representative trace of 4-AP eliciting concentration-dependent relaxation of arterial segments precontracted with NA. (A, panel ii) Mean data of 4-AP-mediated relaxation in NA-precontracted arteries with endothelium intact (Control; $n = 6$) or removed (Denuded; $n = 5$). (B, panel i) Representative trace showing 4-AP-mediated, concentration-dependent contraction of arteries precontracted with 62 mM KPSS ($n = 5$); and (B, panel ii) the accompanying mean data. (C) Concentration–response curves to NA in the absence (Control; $n = 5$) or presence of 1 mM 4-AP ($n = 5$). (D) The effect of increasing concentrations of 4-AP on arteries at rest in the absence and presence of different potassium channel blockers (n = 5–6). Data are mean ± SEM; n = number of arteries from separate animals. *$P < 0.05$ compared to pEC$_{50}$ of within vessel control curve; Student's paired t-test. †$P < 0.05$ compared to control; one-way ANOVA with Dunnett's *post hoc* test.

4-AP is calculated as the difference in tension generated by NA in the absence and presence of 1 mM 4-AP ($T_{NA} - T_{NA+4AP}$); all tension values were normalized to the maximum T_{NA} response. The relationship between the inhibitory effect of 1 mM 4-AP and T_{NA} was calculated in arteries with and without combined K_v7 and BK_{Ca} channel blockade (data from Figures 4C and 9C were used to generate the control and XE991 + IBtx curve, respectively). Figure 9D shows that 1 mM 4-AP can inhibit NA-induced contraction through both K_v7/BK_{Ca} channel activation and inhibition of NA-mediated signal transduction.

Discussion

In this study, we established the direct effect of 4-AP on $K_v7.4$ and $K_v7.5$ channels and characterized its effects on vascular smooth muscle membrane potential, $[Ca^{2+}]_i$, pH_i and tone. Although these data highlight the complex and multifaceted nature of 4-AP to both enhance and inhibit K^+ currents in native systems, we showed that 4-AP, previously regarded as a blocker of K_v7 channels, can enhance K^+ currents in isolated mesenteric artery smooth muscle cells and hyperpolarize vascular smooth muscle, decrease $[Ca^{2+}]_i$ and consequently relax precontracted arteries in a concentration-dependent manner. We further propose that 4-AP can inhibit NA-mediated vasoconstriction by inhibiting NA-induced signal transduction, in part via intracellular alkalization of vascular smooth muscle cells.

For several decades, 4-AP has been used to pharmacologically elucidate the functional impact of K_v1-K_v4 channels in different cell types. For the K_v1-K_v4 channels, the IC_{50}s of 4-AP typically range between 0.1 and 2 mM (Stühmer *et al.*, 1989; Grissmer *et al.*, 1994; Coetzee *et al.*, 1999), although

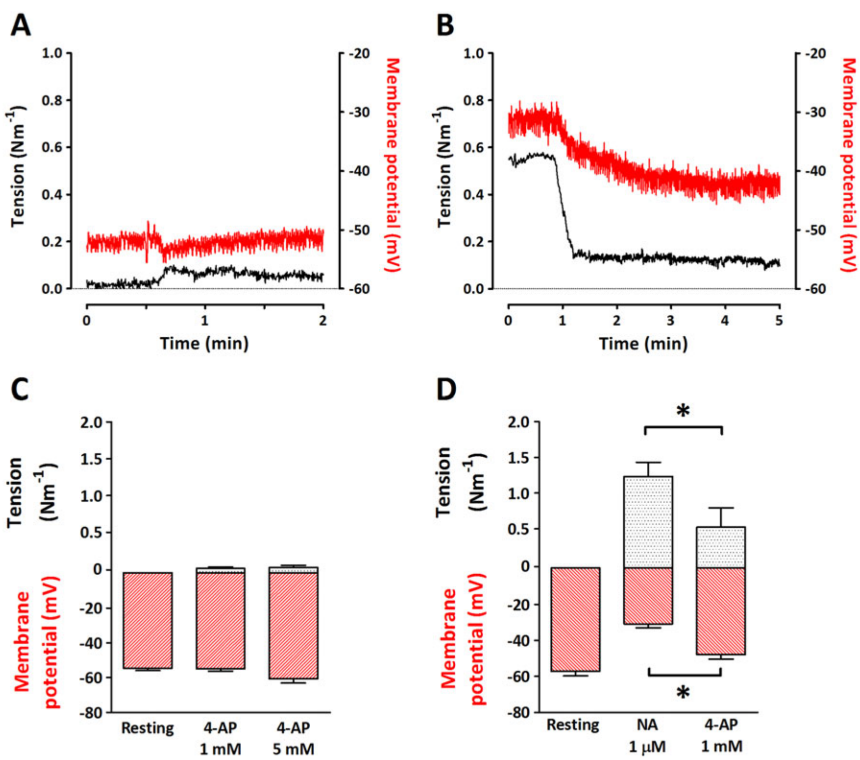

Figure 5

4-AP caused smooth muscle relaxation and membrane hyperpolarization in mesenteric arteries stimulated with NA. (A) Representative trace of tension (black) and membrane potential (red) in response to 1 mM 4-AP in resting arteries (n = 5) and in (B) arteries stimulated with 1 μM NA (n = 6). (C) and (D) Mean data of the steady-state values in (A) and (B) respectively. Data are mean ± SEM; n = number of arteries from separate animals. *$P < 0.05$, comparisons indicated by lines; Student's paired t-test.

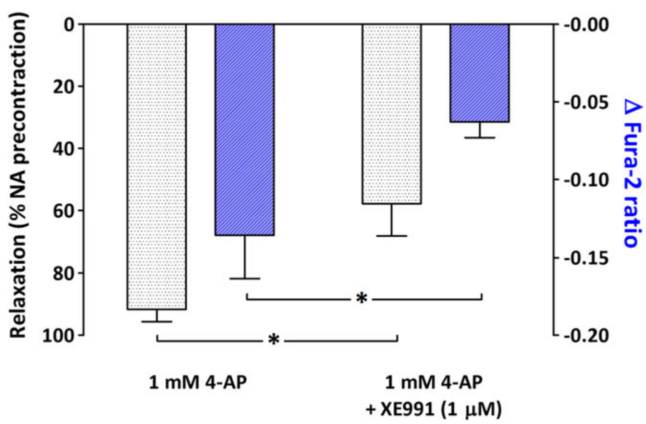

Figure 6

K_v7 channel blockade partially inhibited 4-AP-mediated relaxation and the decrease in $[Ca^{2+}]_i$ in mesenteric arteries. Relaxation-response to 1 mM 4-AP and corresponding changes in the F_{350}/F_{380} ratio (Δ Fura-2 ratio) in arteries precontracted with 1 μM NA in the absence and in the presence of 1 μM XE991 (n=6). Data are mean ± SEM; n = number of arteries from separate rats. *$P < 0.05$, compared to response in the absence of XE991; Student's unpaired t-test.

there are exceptions. **K_v4.1–K_v4.3** and **K_v1.4** channels are 10-fold less sensitive to 4-AP and require up to 13 mM to achieve half-maximal block. In contrast, **K_v3.1** channels appear to be the most sensitive to 4-AP, with an IC_{50} reportedly as low as 0.02 mM (Coetzee *et al.,* 1999). In a review by Coetzee *et al.* (1999), 4-AP was reported to have no effect on **K_v7.1–7.3** channels at concentrations up to 2 mM, although no reference was provided to support these claims. Additionally, currents produced by inner hair cells of the ear, attributed to K_v7.4, were unaffected by 4-AP up to 30 mM (Oliver *et al.,* 2003; Kimitsuki *et al.,* 2010). However, we are unaware of any study that has examined systematically the effect of 4-AP on heterologously expressed K_v7.4 and K_v7.5 channels. In this study, we have used both oocytes and HEK cells to show that 4-AP enhances K_v7.4 currents, and in oocytes over-expressing K_v7.5, 4-AP up to 5 mM had no effect on the currents. Interestingly, in HEK cells, we found that 0.1 and 0.3 mM 4-AP enhanced the K_v7.4 current, whilst concentrations >1 mM inhibited the K_v7.4 current.

K_v7 channels, particularly K_v7.4 and K_v7.5, have been identified in the murine, rat, swine and human vasculature as regulators of vascular reactivity in both conduit and resistance arteries (Yeung *et al.,* 2007; Mackie *et al.,* 2008; Ng *et al.,* 2011; Chadha *et al.,* 2012; Brueggemann *et al.,* 2014; Hedegaard *et al.,* 2014). These α-subunit subtypes are likely to form a K_v7.4/7.5 heteromeric channel in certain arteries (Brueggemann *et al.,* 2014; Chadha *et al.,* 2014). Given the importance of the K_v7.4 and K_v7.5 channels in the vasculature, we aimed to determine the effect of 4-AP on isolated smooth muscle cells and segments of third-order rat mesenteric arteries.

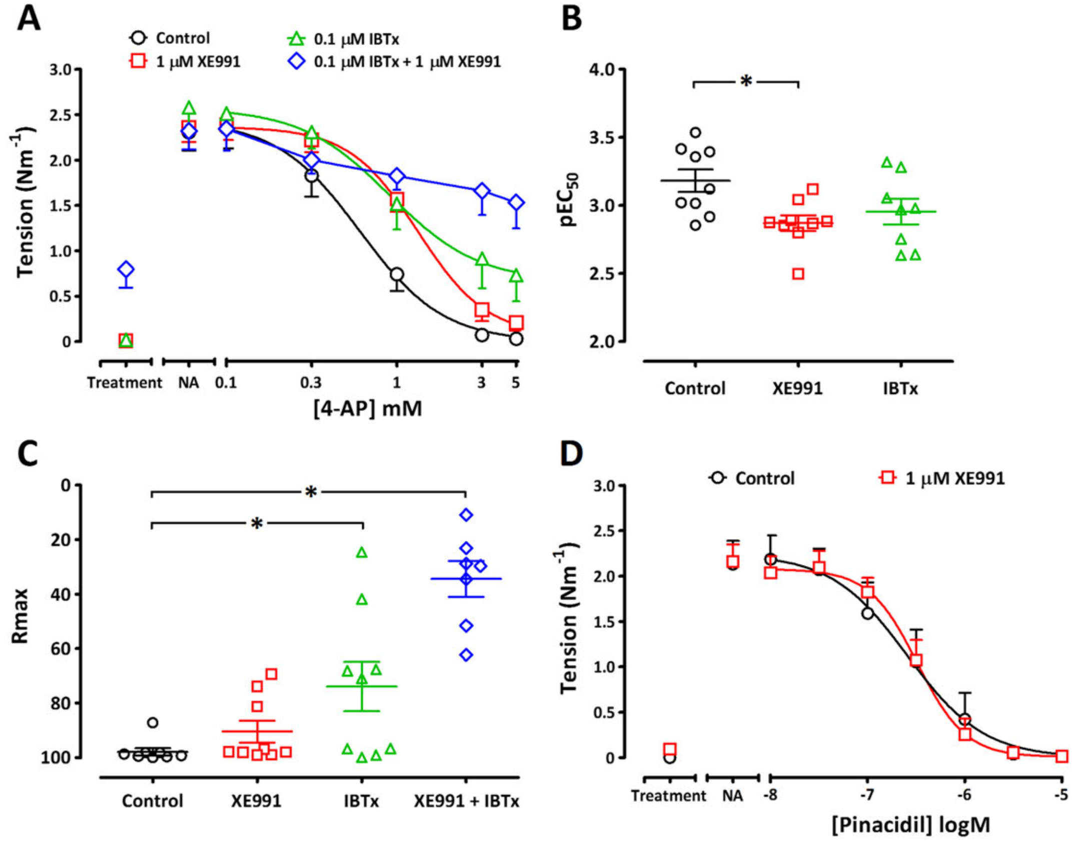

Figure 7

Combined K_v7 and BK_{Ca} channel blockade caused almost complete inhibition of 4-AP-medited relaxation. (A) Concentration–response curves to 4-AP in the presence of various treatments: (i) 0.1% DMSO (Control); (ii) 1 μM XE991; (iii) 0.1 μM iberiotoxin (IBTx) or a combination of (ii) and (iii), in arteries precontracted with NA to approximately 90% of the maximal contraction induced by KPSS. pEC_{50} and Rmax values for 4-AP-induced relaxation are presented in (B) and (C) respectively. In arteries treated with a combination of XE991 and iberiotoxin, 4-AP concentration–response curves often had a poorly defined maximum relaxation plateau: therefore, pEC_{50}s could not be determined for this experimental group. (D) XE991 (1 μM) had no significant effect on the concentration–response curve to pinacidil. Data are mean ± SEM; n = 7–9 for each group. *P < 0.05, one-way ANOVA with Dunnett's *post hoc* test.

In isolated smooth muscle cells, application of 0.1 mM 4-AP increased the K^+ current, whereas in the presence of the K_v7 channel blocker, XE991, 4-AP inhibited the K^+ current. These data show that 4-AP is able to enhance an XE991-sensitive component of the total K^+ current in mesenteric artery smooth muscle cells, whilst also inhibiting an XE991-insensitive component of the current. When applied to NA-precontracted arteries, we found that 4-AP caused concentration-dependent relaxations in an endothelium-independent manner. This relaxation coincided with hyperpolarization of the membrane potential and a reduction in $[Ca^{2+}]_i$, which, in both cases, had been elevated by NA preconstriction. Consistent with this, we found that the NA concentration–response curve was shifted to the right with 1 mM 4-AP, as has been reported previously in rat mesenteric small arteries (Laskowski *et al.,* 2017). In contrast, 4-AP caused contraction in arteries precontracted with high K^+ (62 mM KPSS) and therefore not susceptible to K_v7 channel activation. We found that K_v7 blockade with XE991 decreased the potency of 4-AP. Although one could attribute this to the ability of a K^+-channel blocker to depolarize the membrane potential and functionally antagonize smooth muscle relaxation, the observation that 1 μM XE991 decreased the potency of 4-AP but not the K_{ATP}-channel opener, pinacidil, supports a specific role for K_v7 activation in 4-AP-induced relaxation.

Previous studies have shown that 4-AP elicits contraction in arterial preparations and either inhibits (Ohya *et al.,* 2003; Yeung and Greenwood, 2005; Yeung *et al.,* 2007) or has no effect on delayed rectifier K_v currents (Mackie *et al.,* 2008; Mani *et al.,* 2013). However, these studies only used concentrations >1 mM 4-AP and did not assess the effect of 4-AP in precontracted arteries. In this study, we also observed a small contraction with 5 mM 4-AP consistent with its effect to inhibit delayed rectifier K_v currents. Given the still somewhat unknown and varied K_v7 channel subtype expression, channel stoichiometry across vascular beds (Jepps *et al.,* 2014) and coassembly with β-subunits (Jepps *et al.,* 2015; Abbott and Jepps, 2016), it is possible that 4-AP is less able to relax other arteries that are more dependent on K_v1, K_v2 or $K_v7.5$ activities, instead inducing a contractile response at concentrations >1 mM. We suggest that the complexity of different native systems together with the multifarious

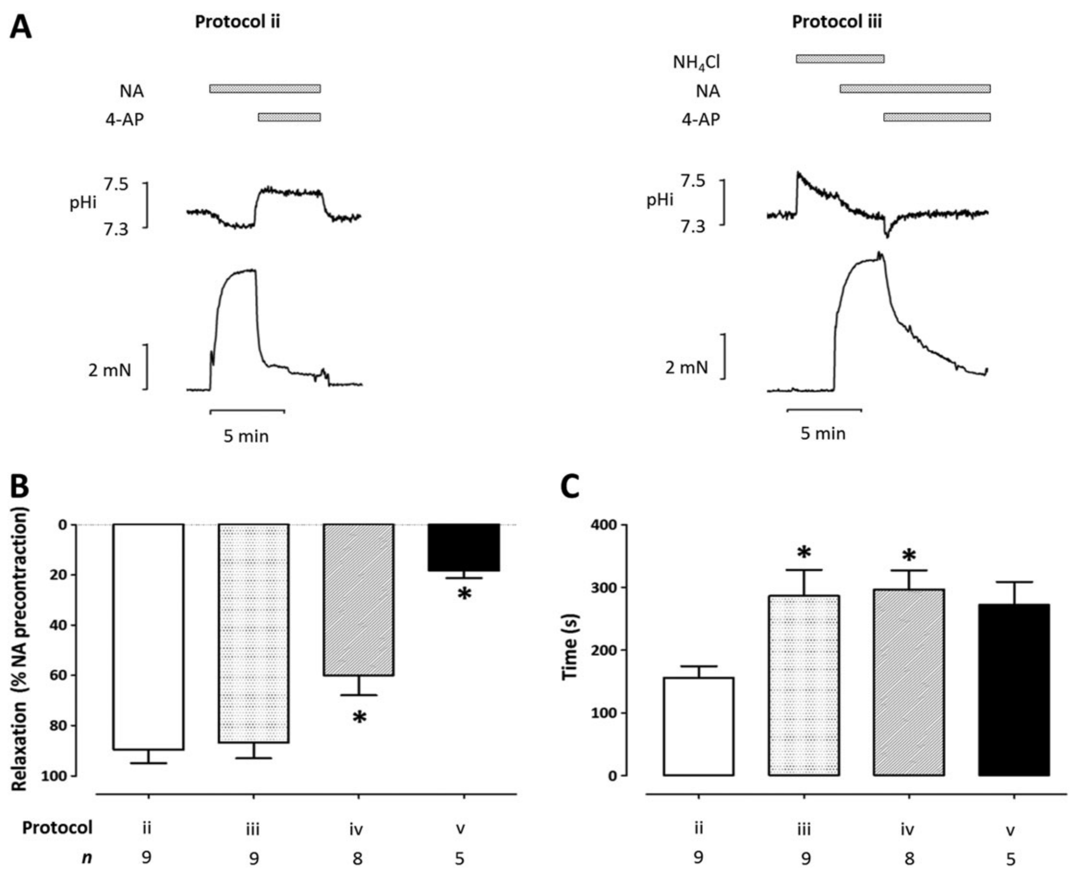

Figure 8

4-AP elevated pH_i, but this alkalization was not required for 4-AP to elicit relaxation. (A) Recording of pH_i (upper trace) and force (lower trace) in a rat mesenteric resistance artery in response to 1 mM 4-AP without (protocol ii) and with NH_4Cl preincubation (protocol iii). (B) Maximum relaxation and (C) time taken for 1 mM 4-AP-mediated relaxation of NA-precontracted arteries to plateau without (protocol ii) and with preincubation with NH_4Cl (protocol iii). Protocol iii was repeated in the presence of 1 μM XE991 (protocol iv) and with the combination of 1 μM XE991 and 0.1 μM iberiotoxin (protocol v). Data are mean ± SEM; n = number of arteries from separate animals. *$P < 0.05$, compared to control 1 mM 4-AP response (protocol ii); one-way ANOVA with Dunnett's *post hoc* test.

nature of 4-AP, particularly at higher concentrations, is responsible for any discrepancies with previous studies.

Notably, K_v7 blockade did not completely inhibit 4-AP-mediated relaxation. We, therefore, speculated that 4-AP must be eliciting relaxation through an additional mechanism. In rat arterial smooth muscle cells, 4-AP enhanced BK_{Ca} currents by increasing pH_i in the presence of BAPTA (Petkova-Kirova *et al.,* 2000). In line with this, we found that iberiotoxin decreased the maximal efficacy of 4-AP-mediated relaxation. When XE991 was present, iberiotoxin almost completely abolished 4-AP-mediated relaxations. These data show that 4-AP-mediated relaxations occur, at least in part, through the activation of K_v7 channels and either a direct or indirect enhancement of BK_{Ca} channel activity. Another possible explanation is the nonlinear relationship between K^+-conductance and membrane potential inherent in the biophysics of membrane electrophysiology (Coleman *et al.*, 2017), which would make a 'second' K^+-conductance inhibitor appear more effective than the 'first' K^+-conductance inhibitor.

Previous studies have reported that 4-AP is able to cross the cell membrane and bind intracellular protons resulting in the formation of $4\text{-}APH^+$ and intracellular alkalization (Choquet and Korn, 1992). To determine whether the 4-AP enhancement of $K_v7.4$ was pH-dependent, we measured pH_i in oocytes. Much like NH_4Cl (Lee and Choi, 2011), we found that 4-AP was unable to change pH_i in ooyctes, suggesting that the enhancement of the $K_v7.4$ channel is pH-independent. Furthermore, although 1 mM 4-AP increased pH_i in mesenteric arteries, the magnitude of 4-AP-induced relaxation was unchanged when alkalization was prevented, although the rate of relaxation was significantly slower. Thus, although 4-AP-induced relaxation does not necessitate an increase in pH_i, the rate of relaxation is facilitated by alkalization. Whether this is mediated via an effect of pH_i on BK_{Ca}, as suggested by Schubert *et al.* (2001) or to an effect of pH_i on $K_v7.4$ is difficult to know. Certainly, in the absence of intracellular alkalization, the relaxation to 4-AP was still attenuated by both XE991 and iberiotoxin.

4-AP also elicited relaxation of NA-precontracted arteries by inhibiting NA-mediated signal transduction independently of $K_v7.4$ activation. In arteries exposed to a 125 mM K^+ and therefore immune to changes in potassium conductance, 4-AP partially relaxed contraction elicited by NA

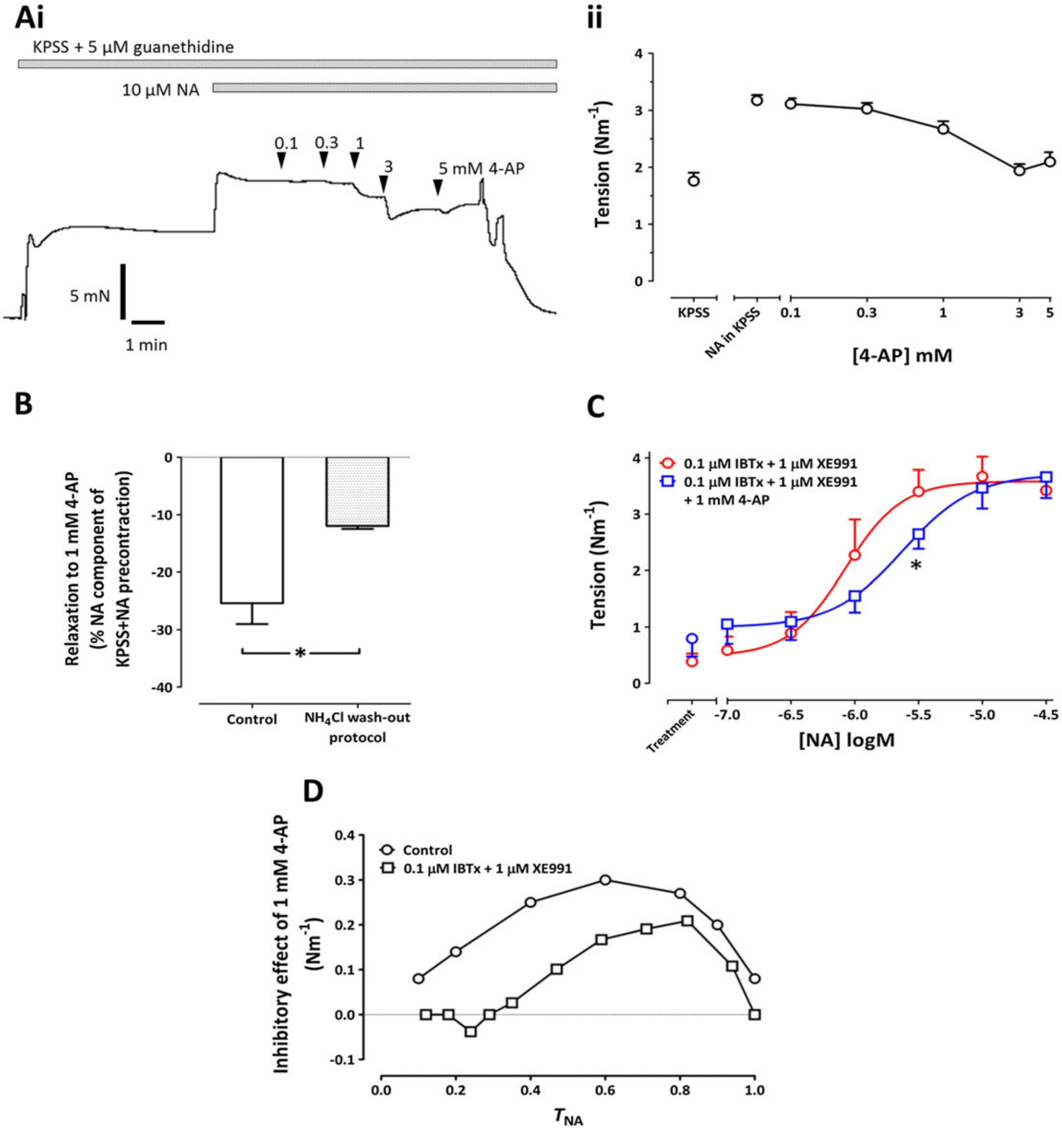

Figure 9

4-AP relaxes mesenteric arteries through three mechanisms: (i) pH_i-dependent- and independent-mediated inhibition of NA-induced signalling; (ii), K_v7 channel activation and (iii), BK_{Ca} channel activation. (A, panel i) Representative trace of 4-AP eliciting concentration-dependent relaxation of arterial segments precontracted with 125 mM KPSS and 10 μM NA and (A, panel ii) the accompanying mean data (n = 5). (B) In arteries precontracted with 125 mM KPSS and then NA (10 μM), prevention of 4-AP-induced changes in pH_i using the NH_4Cl washout protocol, partially inhibited the relaxation response to 1 mM 4-AP (expressed as a percentage of the additional contraction elicited by NA on top of 125 mM KPSS; n = 5, $^*P < 0.05$ compared to control; Student's paired t-test). (C) Cumulative concentration–response curves to NA following K_v7 and BK_{Ca} channel blockade in the absence and presence of 1 mM 4-AP (n = 5). Data are mean ± SEM; n = number of arteries from separate animals. $^*P < 0.05$ compared to pEC$_{50}$ of within vessel control curve; Student's paired t-test. (D) Inhibitory effect of 1 mM 4-AP expressed as the difference in tension generated by NA in the absence and presence of 1 mM 4-AP ($T_{NA} - T_{NA+4AP}$); all tension values were normalized to the maximum T_{NA} response so that maximum T_{NA} = 1. The relationship between the inhibitory effect of 1 mM 4-AP and T_{NA} was calculated in arteries with and without 0.1 μM IBTx and 1 μM XE991 (refer to results section for details).

(Figure 9A). 4-AP also caused a rightward shift of the NA-concentration-response curves generated in the presence of K_v7 and BK_{Ca} blockade (Figure 9C). Inhibition of NA-induced signalling appears to be partly due to 4-AP-induced intracellular alkalization since the capacity of 1 mM 4-AP to elicit relaxation of a NA-induced contractile component was markedly reduced when changes in pH_i were prevented. This is unlike the observations observed in arteries precontracted with a submaximal concentration of NA where intracellular alkalization affected the rate but not the magnitude of 4-AP-induced relaxation. This difference in pH_i dependency highlights the varying contribution of (i) K_v activation; (ii) BK_{Ca} activation; and (iii) inhibition of NA-mediated signalling to 4-AP-induced relaxation at different levels of NA-induced tension. Figure 9D highlights the K_v7 and BK_{Ca} sensitive and insensitive parts of the relaxation to 4-AP as a function of the tension generated by NA and reinforces the conclusion, based on the comparison of the effect of XE991 on 4-AP- and pinacidil-induced relaxation that 4-AP is able to activate K_v7 channels in intact mesenteric arteries to partially mediate relaxation.

In summary, this study shows, first and foremost, that 4-AP can enhance K_v7.4 channel activity. When we applied 4-AP to NA-preconstricted rat mesenteric arteries, we found that 4-AP has several mechanisms of action that can result in a relaxation of the vessel, namely, (i) activation of K_v7.4 channels, (ii) activation of BK_{Ca} channels either directly or indirectly, and (iii) attenuation of NA-signalling, which is partly pH_i-dependent. Taken together, these findings provide a crucial understanding of the complex nature effect of 4-AP in native systems, such as vascular smooth muscle cells. It is clear from this study that results obtained using 4-AP in arterial, and possibly other, smooth muscle preparations will be difficult to interpret due to the mixed inhibition and enhancement of different potassium channels and its potential to inhibit NA-induced signalling pathways. This work cautions against using 4-AP as a general inhibitor of K_v channels and questions the appropriateness of using 4-AP to dissect out the functional contributions of K_v7 channels from other K_v channels.

Clinical significance

Clinically, 4-AP is used to treat multiple sclerosis under the trade name AMPYRA® (dalfampridine). This drug has many reported side effects, several of which may involve the direct alteration of smooth muscle activity, such as dizziness (reduced cerebral blood flow), vascular pain, constipation and renal impairment (Jensen *et al.*, 2014; Fujihara and Miyoshi, 1998). This study improves our understanding of 4-AP and highlights the multitude of pathways that can be affected by this compound in native systems, particularly regarding smooth muscle function, which may account for some of the side effects from AMPYRA.

Acknowledgements

We are grateful to Amer Mujezinovic (University of Copenhagen) for performing the two-electrode voltage clamp experiments. T.A.J. received funding from the Carlsberg Foundation (CF16-0136) and the Lundbeck Foundation (R181-2014-4030). M.M.K. was supported by a Novo Nordic Foundation Grant (11789) awarded to C.A.

Author contributions

M.M.K. performed experiments, analysed data and drafted the manuscript. T.A.J. performed experiments, analysed data and contributed to manuscript writing and funding provision. C.A. contributed to experimental design, manuscript writing and funding provision. S.K., S.L. and I.C. all performed experiments and analysed data. B.H.B. designed experiments, analysed data and contributed to drafting the manuscript.

Conflicts of interest

The authors declare no conflicts of interest.

Declaration of transparency and scientific rigour

This Declaration acknowledges that this paper adheres to the principles for transparent reporting and scientific rigour of preclinical research recommended by funding agencies, publishers and other organisations engaged with supporting research.

References

Aalkjaer C, Cragoe EJ Jr (1988). Intracellular pH regulation in resting and contracting segments of rat mesenteric resistance vessels. J Physiol 402: 391.

Abbott GW, Jepps TA (2016). Kcne4 deletion sex-dependently alters vascular reactivity. J Vasc Res 53: 138–148.

Albarwani S, Nemetz LT, Madden JA, Tobin AA, England SK, Pratt PF *et al.* (2003). Voltage-gated K+ channels in rat small cerebral arteries: molecular identity of the functional channels. J Physiol 551: 751–763.

Alexander SPH, Striessnig J, Kelly E, Marrion NV, Peters JA, Faccenda E *et al.* (2017). The Concise Guide to PHARMACOLOGY 2017/18: Voltage-gated ion channels. Br J Pharmacol 174: S160–S194.

Brueggemann LI, Mackie AR, Cribbs LL, Freda J, Tripathi A, Majetschak M *et al.* (2014). Differential protein kinase C-dependent modulation of Kv7.4 and Kv7.5 subunits of vascular Kv7 channels. J Biol Chem 289: 2099–2111.

Chadha PS, Zunke F, Davis AJ, Jepps TA, Linders JTM, Schwake M *et al.* (2012). Pharmacological dissection of Kv7.1 channels in systemic and pulmonary arteries. Br J Pharmacol 166: 1377–1387.

Chadha PS, Jepps TA, Carr G, Stott JB, Zhu HL, Cole WC *et al.* (2014). Contribution of k_v7.4/k_v7.5 heteromers to intrinsic and calcitonin gene-related peptide-induced cerebral reactivity. Arterioscler Thromb Vasc Biol 34: 887–893.

Choquet D, Korn H (1992). Mechanism of 4-aminopyridine action on voltage-gated potassium channels in lymphocytes. J Gen Physiol 99: 217.

Coetzee WA, Amarillo Y, Chiu J, Chow A, Lau D, McCormack TOM *et al.* (1999). Molecular diversity of K+ channels. Ann N Y Acad Sci 868: 233–255.

Coleman HA, Tare M, Parkington HC (2017). Nonlinear effects of potassium channel blockers on endothelium-dependent hyperpolarization. Acta Physiol (Oxf) 219: 324–334.

Cox RH, Fromme SJ, Folander KL, Swanson RJ (2008). Voltage gated K+ channel expression in arteries of Wistar–Kyoto and spontaneously hypertensive rats. Am J Hypertens 21: 213–218.

Curtis MJ, Bond RA, Spina D, Ahluwalia A, Alexander S, Giembycz MA *et al.* (2015). Experimental design and analysis and their reporting: new guidance for publication in BJP. Br J Pharmacol 172: 3461–3471.

Fergus DJ, Martens JR, England SK (2003). Kv channel subunits that contribute to voltage-gated K+ current in renal vascular smooth muscle. Pflugers Arch 445: 697–704.

Fujihara K, Miyoshi T (1998). The effects of 4-aminopyridine on motor evoked potentials in multiple sclerosis. J Neurol Sci 159: 102–106.

Grissmer S, Nguyen AN, Aiyar J, Hanson DC, Mather RJ, Gutman GA *et al*. (1994). Pharmacological characterization of five cloned voltage-gated K+ channels, types Kv1. 1, 1.2, 1.3, 1.5, and 3.1, stably expressed in mammalian cell lines. Mol Pharmacol 45: 1227–1234.

Hedegaard ER, Nielsen BD, Kun A, Hughes AD, Krøigaard C, Mogensen S *et al*. (2014). Kv7 channels are involved in hypoxia-induced vasodilatation of porcine coronary arteries. Br J Pharmacol 171: 69–82.

Jensen HB, Ravnborg M, Dalgas U, Stenager E (2014). 4-Aminopyridine for symptomatic treatment of multiple sclerosis: a systematic review. Ther Adv Neurol Disord 7: 97–113.

Jepps TA, Bentzen BH, Stott JB, Povstyan OV, Sivaloganathan K, Dalby-Brown W *et al*. (2014). Vasorelaxant effects of novel Kv7.4 channel enhancers ML213 and NS15370. Br J Pharmacol 171: 4413–4424.

Jepps TA, Carr G, Lundegaard PR, Olesen SP, Greenwood IA (2015). Fundamental role for the KCNE4 ancillary subunit in Kv7.4 regulation of arterial tone. J Physiol 593: 5325–5340.

Kilkenny C, Browne W, Cuthill IC, Emerson M, Altman DG (2010). Animal research: reporting *in vivo* experiments: the ARRIVE guidelines. Br J Pharmacol 160: 1577–1579.

Kimitsuki T, Komune N, Noda T, Takaiwa K, Ohashi M, Komune S (2010). Property of I_{Kn} in inner hair cells isolated from guinea-pig cochlea. Hear Res 261: 57–62.

Laskowski M, Andersson C, Eliasson E, Golubinskaya V, Nilsson H (2017). Potassium-channel-independent relaxing influence of adipose tissue on mouse carotid artery. J Vasc Res 54: 51–57.

Lee S, Choi I (2011). Sodium-bicarbonate cotransporter NBCn1/Slc4a7 inhibits NH_4Cl-mediated inward current in Xenopus oocytes. Exp Physiol 96: 745–755.

Lee HJ, Kwon MH, Lee S, Hall RA, Yun CC, Choi I (2014). Systematic family-wide analysis of sodium bicarbonate cotransporter NBCn1/SLC4A7 interactions with PDZ scaffold proteins. Physiol Rep 20: 2.

Mackie AR, Brueggemann LI, Henderson KK, Shiels AJ, Cribbs LL, Scrogin KE *et al*. (2008). Vascular KCNQ potassium channels as novel targets for the control of mesenteric artery constriction by vasopressin, based on studies in single cells, pressurized arteries, and *in vivo* measurements of mesenteric vascular resistance. J Pharmacol Exp Ther 325: 475–483.

Mani BK, O'Dowd J, Kumar L, Brueggemann LI, Ross M, Byron KL (2013). Vascular KCNQ (Kv7) potassium channels as common signaling intermediates and therapeutic targets in cerebral vasospasm: Kv7 channel openers to treat cerebral vasospasm. J Cardiovasc Pharmacol 61: 51.

McGrath JC, Lilley E (2015). Implementing guidelines on reporting research using animals (ARRIVE etc.): new requirements for publication in BJP. Br J Pharmacol 172: 3189–3193.

Mulvany MJ, Halpern W (1977). Contractile properties of small arterial resistance vessels in spontaneously hypertensive and normotensive rats. Circ Res 41: 19–26.

Mulvany MJ, Nilsson H, Flatman JA (1982). Role of membrane potential in the response of rat small mesenteric arteries to exogenous noradrenaline stimulation. J Physiol 332: 363.

Ng FL, Davis AJ, Jepps TA, Harhun MI, Yeung SY, Wan A *et al*. (2011). Expression and function of the K+ channel KCNQ genes in human arteries. Br J Pharmacol 162: 42–53.

Ohya S, Sergeant GP, Greenwood IA, Horowitz B (2003). Molecular variants of KCNQ channels expressed in murine portal vein myocytes. Circ Res 92: 1016–1023.

Oliver D, Knipper M, Derst C, Fakler B (2003). Resting potential and submembrane calcium concentration of inner hair cells in the isolated mouse cochlea are set by KCNQ-type potassium channels. J Neurosci 23: 2141–2149.

Petkova-Kirova P, Gagov H, Krien U, Duridanova D, Noack T, Schubert R (2000). 4-Aminopyridine affects rat arterial smooth muscle BKCa currents by changing intracellular pH. Br J Pharmacol 131: 1643–1650.

Robbins J (2001). KCNQ potassium channels: physiology, pathophysiology, and pharmacology. Pharmacol Ther 90: 1–19.

Schubert R, Krien U, Gagov H (2001). Protons inhibit the BKCa channel of rat small artery smooth muscle cells. JVR 38: 30–38.

Southan C, Sharman JL, Benson HE, Faccenda E, Pawson AJ, Alexander SPH *et al*. (2016). The IUPHAR/BPS guide to PHARMACOLOGY in 2016: towards curated quantitative interactions between 1300 protein targets and 6000 ligands. Nucl Acids Res 44: D1054–D1068.

Stott JB, Jepps TA, Greenwood IA (2014). KV7 potassium channels: a new therapeutic target in smooth muscle disorders. Drug Discov Today 19: 413–424.

Stühmer W, Ruppersberg JP, Schröter KH, Sakmann B, Stocker M, Giese KP *et al*. (1989). Molecular basis of functional diversity of voltage-gated potassium channels in mammalian brain. EMBO J 8: 3235–3244.

Thomas JA, Buchsbaum RN, Zimniak A, Racker E (1979). Intracellular pH measurements in Ehrlich ascites tumor cells utilizing spectroscopic probes generated in situ. Biochemistry (Mosc) 18: 2210–2218.

Wulff H, Castle NA, Pardo LA (2009). Voltage-gated potassium channels as therapeutic targets. Nat Rev Drug Discov 8: 982–1001.

Yeung SYM, Greenwood IA (2005). Electrophysiological and functional effects of the KCNQ channel blocker XE991 on murine portal vein smooth muscle cells. Br J Pharmacol 146: 585–595.

Yeung SYM, Pucovský V, Moffatt JD, Saldanha L, Schwake M, Ohya S *et al*. (2007). Molecular expression and pharmacological identification of a role for Kv7 channels in murine vascular reactivity. Br J Pharmacol 151: 758–770.

Supporting Information

Additional Supporting Information may be found online in the supporting information tab for this article.

https://doi.org/10.1111/bph.14097

Figure S1 4-AP-mediated inhibition of NA-induced contraction is independent of Kv7 channel and/or BKCa channel activation.
Figure S2 In the presence of nifedipine, 4-AP does not relax mesenteric arteries precontracted with U46619.